



# Upward expansion and acceleration of forest clearance in the mountains of Southeast Asia

Yu Feng  <sup>1,2</sup>, Alan D. Ziegler<sup>3</sup>, Paul R. Elsen  <sup>4</sup>, Yang Liu<sup>1</sup>, Xinyue He  <sup>1,5</sup>, Dominick V. Spracklen<sup>5</sup>, Joseph Holden  <sup>6</sup>, Xin Jiang<sup>1</sup>, Chunmiao Zheng  <sup>1</sup> and Zhenzhong Zeng  <sup>1</sup>✉

**Southeast Asia contains about half of all tropical mountain forests, which are rich in biodiversity and carbon stocks, yet there is debate as to whether regional mountain forest cover has increased or decreased in recent decades. Here, our analysis of high-resolution satellite datasets reveals increasing mountain forest loss across Southeast Asia. Total mean annual forest loss was  $3.22 \text{ Mha yr}^{-1}$  during 2001–2019, with 31% occurring on the mountains. In the 2010s, the frontier of forest loss moved to higher elevations ( $15.1 \pm 3.8 \text{ m yr}^{-1}$  during 2011–2019,  $P < 0.01$ ) and steeper slopes ( $0.22 \pm 0.05^\circ \text{ yr}^{-1}$  during 2009–2019,  $P < 0.01$ ) that have high forest carbon density relative to the lowlands. These shifts led to unprecedented annual forest carbon loss of  $424 \text{ Tg C yr}^{-1}$ , accelerating at a rate of  $18 \pm 4 \text{ Tg C yr}^{-2}$  ( $P < 0.01$ ) from 2001 to 2019. Our results underscore the immediate threat of carbon stock losses associated with accelerating forest clearance in Southeast Asian mountains, which jeopardizes international climate agreements and biodiversity conservation.**

Tropical forests are the largest terrestrial component of the global carbon cycle<sup>1</sup>, storing 247 Pg C in above- and below-ground biomass<sup>2</sup>. However, recent anthropogenic-influenced forest loss has reshaped tropical forests profoundly<sup>3</sup>, weakening their ability to store carbon and regulate climate<sup>4</sup>. Currently, across the tropics, the amount of carbon sequestered by intact forests and forest regrowth is approximately similar to that released from forest loss, suggesting that tropical forests probably act as a neutral contributor to the global carbon cycle<sup>5</sup>. Forest loss in the tropics, which dominates the total loss worldwide in the twenty-first century<sup>6–10</sup>, has been driven largely by agricultural intensification and/or extensification to support demands for human/animal food trade, profit-driven (illegal) logging and other activities that are inherently linked to population growth<sup>11–13</sup>. Of concern is that acceleration of forest clearance in the future will intensify carbon stock loss, potentially transforming tropical forests into important net carbon sources<sup>5,14,15</sup>, as well as disrupting biodiversity patterns, human livelihoods, hydro-geomorphological processes and ecosystem functions.

The general notion is that tropical deforestation worldwide occurs primarily in lowland areas. This sentiment aligns with previous work showing substantial forest losses at low elevations but only negligible losses, and even some forest gains, in the mountains<sup>6,16,17</sup>. However, in Southeast Asia (SEA), where approximately half of the world's tropical mountain forests are located<sup>8,18</sup> and extensive forest losses in the lowlands of Indonesia have occurred<sup>6,9</sup>, recent studies have reported new croplands and plantations replacing mountain forests in Laos and Thailand of montane mainland SEA<sup>19,20</sup>. Yet the applicability of these results<sup>19,20</sup> as an indicator of a regional trend is debatable, as some global analyses<sup>7,17</sup> indicate an increase in forest cover in this region. New spatiotemporal analyses conducted at high resolution and with common vegetation definitions are needed to address these inconsistencies related to topography of forest loss in the mountains and lowlands of SEA.

In this article, we analyse multiple high-resolution satellite datasets to provide a comprehensive assessment of changes in topographical patterns of forest clearance and related carbon loss across SEA during the first two decades of the twenty-first century. The analyses incorporate the global mountain-extent map<sup>18</sup> with two 30-m-resolution products reporting the global forest-cover change<sup>8</sup> and aboveground live woody biomass (AGB) density<sup>21</sup> (Methods). Owing to limitations of distinguishing tree types in the satellite products used<sup>8</sup>, unless specifically stated, 'forest losses' incorporate those from primary forest, secondary forest disturbance and tree-dominated plantations, including oil palm and rubber. As the mountains of SEA hold more forest biomass carbon than lowlands<sup>22</sup> (Supplementary Fig. 1), a better understanding of forest and related biomass carbon dynamics is crucial for reducing uncertainties in the global carbon cycle, as well as guiding land management in the region.

## Results

This section presents our findings of forest loss in SEA, including the patterns of forest loss and related topography and carbon loss.

**Accelerating forest loss and related topography.** We find a total forest loss of 61 Mha in SEA during the period 2001–2019, which is equivalent to a rate of  $3.22 \text{ Mha yr}^{-1}$  (Table 1, Fig. 1a and Supplementary Fig. 2c). Annual forest loss of the 2010s ( $4.02 \text{ Mha yr}^{-1}$ ) was nearly twice that of the 2000s ( $2.33 \text{ Mha yr}^{-1}$ ), with the greatest loss occurring in 2016 ( $5.79 \text{ Mha yr}^{-1}$ ). Approximately 31% of the loss during the 19-year period (19 Mha;  $1.00 \text{ Mha yr}^{-1}$ ) occurred within the 61 mountains that occupy 1.7 million km<sup>2</sup> of the region (38% of SEA's land surface; Supplementary Fig. 2a,c). We also find a significant increase in annual forest-loss area across SEA since 2001, with an acceleration rate of  $0.17 \pm 0.03 \text{ Mha yr}^{-2}$  ( $P < 0.01$ ). The annual rate of mountain forest loss increased 2.4-fold from  $0.58 \text{ Mha yr}^{-1}$  in the first decade to  $1.38 \text{ Mha yr}^{-1}$  in the second decade (Fig. 1a).

<sup>1</sup>State Environmental Protection Key Laboratory of Integrated Surface Water–Groundwater Pollution Control, School of Environmental Science and Engineering, Southern University of Science and Technology, Shenzhen, China. <sup>2</sup>Department of Civil Engineering, The University of Hong Kong, Hong Kong, China. <sup>3</sup>Faculty of Fisheries Technology and Aquatic Resources, Mae Jo University, Chiang Mai, Thailand. <sup>4</sup>Wildlife Conservation Society, Global Conservation Program, Bronx, NY, USA. <sup>5</sup>School of Earth and Environment, University of Leeds, Leeds, UK. <sup>6</sup>School of Geography, University of Leeds, Leeds, UK. ✉e-mail: [zengzz@sustech.edu.cn](mailto:zengzz@sustech.edu.cn)

**Table 1 | Forest and related carbon loss in the mountains and lowlands of SEA**

| Variables   | Year range | All forests |           |          | Primary forests |           |          | Secondary forests |           |
|---|------------|-------------|-----------|----------|-----------------|-----------|----------|-------------------|-----------|
|   |            | SEA         | Mountains | Lowlands | SEA             | Mountains | Lowlands | SEA               | Mountains |
| Gross forest loss (Mha yr <sup>-1</sup> )                         | 2001-2019  | 3.22        | 1.00      | 2.22     | 0.93            | 0.26      | 0.67     | 2.29              | 0.74      |
|   | 2001-2009  | 2.33        | 0.58      | 1.76     | 0.72            | 0.18      | 0.54     | 1.61              | 0.40      |
|   | 2010-2019  | 4.02        | 1.38      | 2.64     | 1.11            | 0.33      | 0.78     | 2.91              | 1.05      |
| Gross forest gain (Mha yr <sup>-1</sup> )                         | 2001-2019  | 1.32        | 0.34      | 0.98     | N.A.            | N.A.      | N.A.     | 1.32              | 0.34      |
| Gross forest carbon loss (Tg C yr <sup>-1</sup> )                 | 2001-2019  | 424         | 136       | 288      | 167             | 48        | 119      | 257               | 88        |
|   | 2001-2009  | 330         | 88        | 242      | 128             | 33        | 95       | 202               | 55        |
|   | 2010-2019  | 508         | 179       | 329      | 202             | 62        | 140      | 306               | 117       |
| Forest-loss acceleration (10 <sup>-2</sup> Mha yr <sup>-2</sup> ) | 2001-2019  | 17±3*       | 8±1*      | 9±2*     | 4±1*            | 2±0*      | 2±1      | 14±2*             | 7±1*      |
|   | 2001-2009  | 26±5*       | 6±1*      | 20±4*    | 11±2*           | 2±0*      | 9±1*     | 15±4*             | 3±1*      |
|   | 2010-2019  | 10±9        | 11±3*     | -1±7     | -5±3            | 1±1       | -5±2     | 15±6*             | 10±2*     |
| Forest carbon loss acceleration (Tg C yr <sup>-2</sup> )          | 2001-2019  | 18±4*       | 10±1*     | 8±3*     | 7±2*            | 3±0*      | 4±2      | 11±2*             | 7±1*      |
|   | 2001-2009  | 35±7*       | 8±2*      | 27±5*    | 19±3*           | 4±1*      | 15±2*    | 16±5*             | 4±1*      |
|   | 2010-2019  | 1±12        | 10±4*     | -9±8     | -7±6            | 1±2       | -9±4     | 8±6               | 9±2*      |
| Trend in mean elevation (10 <sup>-1</sup> m yr <sup>-1</sup> )    | 2001-2019  | 64±13*      | 46±15*    | 16±3*    | 50±17*          | 16±16     | 27±7*    | 52±11*            | 38±11*    |
|   | 2001-2011  | 1±19        | 11±28     | 0±5      | -56±15*         | -66±23*   | -16±9    | 8±18              | 20±23     |
|   | 2011-2019  | 151±38*     | 95±57*    | 37±10*   | 195±30*         | 127±46*   | 85±16*   | 113±37*           | 62±46*    |
| Trend in mean slope (10 <sup>-2</sup> deg yr <sup>-1</sup> )      | 2001-2019  | 11±2*       | 12±2*     | 3±1*     | 11±3*           | 6±3*      | 8±2*     | 9±2*              | 11±2*     |
|   | 2001-2009  | -4±3        | 1±5       | -2±0     | -17±0*          | -14±0*    | -9±0*    | -4±0              | 2±4       |
|   | 2009-2019  | 22±5*       | 20±8*     | 7±2      | 31±7*           | 21±8*     | 19±6*    | 19±5*             | 17±7*     |

\*Statistically significant trend at the level of  $P < 0.05$ . N.A., not applicable.

Forest loss occurring in the lowlands of SEA significantly accelerated only during the 2000s ( $0.20 \pm 0.04 \text{ Mha yr}^{-2}$ ,  $P < 0.01$ ), with a non-significantly decreasing trend in the following decade ( $-0.01 \pm 0.07 \text{ Mha yr}^{-2}$ ,  $P = 0.92$ ). This pattern mirrors the fact that there were limited lowland forests that could be converted to croplands in some regions over SEA during the 2010s, as lowland forests had continued to be cleared since the 1980s<sup>6</sup>. Regarding mountain forest loss, the near doubling of acceleration rates from the first ( $0.06 \pm 0.01 \text{ Mha yr}^{-2}$ ,  $P < 0.01$ ) to the second ( $0.11 \pm 0.03 \text{ Mha yr}^{-2}$ ,  $P < 0.01$ ) decade resulted from accelerated conversion of forests for crop plantation in the mountains<sup>19</sup>. Further, the trend in lowland forest loss was significantly different from that in the mountains during the 2000s ( $P < 0.05$ ), but this difference was no longer statistically significant during the 2010s (Fig. 1a). Taken together, these patterns reveal that forest loss in the mountains increasingly made up a substantial portion of total forest loss in SEA from 2001 (24%) to 2019 (42%), which is a new finding<sup>6,9,23</sup>.

Incorporating data on primary forest extent in 2001<sup>10</sup>, we further estimate that annual loss of primary forest from 2001 to 2019 was  $0.93 \text{ Mha yr}^{-1}$  (Table 1 and Supplementary Fig. 3), with  $0.26 \text{ Mha yr}^{-1}$  (28%) occurring in the mountains and  $0.67 \text{ Mha yr}^{-1}$  (72%) in the lowlands. These equate to 2.9% and 7.3% losses of the primary forest extent in 2001. Throughout the 19-year period, secondary forest loss always exceeded primary forest loss in both the lowlands and the mountains. Whereas secondary forest loss accelerated significantly throughout the whole period ( $0.14 \pm 0.02 \text{ Mha yr}^{-2}$ ,  $P < 0.01$ ), the significant acceleration in primary forest loss in the first decade ( $0.11 \pm 0.02 \text{ Mha yr}^{-2}$ ,  $P < 0.01$ ) gave way to a non-significant decline in primary forest loss in the second decade ( $-0.05 \pm 0.03 \text{ Mha yr}^{-2}$ ,  $P = 0.19$ ). Two trends emerged during the 2010s: (1) secondary forest loss in the mountains greatly increased ( $0.10 \pm 0.02 \text{ Mha yr}^{-2}$ ,  $P < 0.05$ ) and (2) primary forest loss in the lowlands non-significantly decreased ( $-0.05 \pm 0.02 \text{ Mha yr}^{-2}$ ,  $P = 0.06$ ). As the trend in

secondary forest loss is much larger than that of primary forest loss over the 19-year period, the ratio of primary-to-total forest loss decreased from  $>30\%$  to 20%. Collectively, the increase in mountain forest loss in the 2010s originated primarily from secondary forest loss, while the overall reduction in primary forest loss resulted from reductions in the lowlands.

An elevational shift in the frontier of forest loss in the region is further supported by changes in the elevation and slope of mean forest loss midway through the 19-year study period (Fig. 1b). Piecewise regression reveals an inflection point (IP) for mean elevation of forest loss that occurred in 2011 and an IP for mean slope of forest loss that occurred in 2009 (Fig. 1b). Within the period after the IPs, the mean elevation and slope increased significantly at rates of  $15.1 \pm 3.8 \text{ m yr}^{-1}$  ( $P < 0.01$ ) and  $0.22 \pm 0.05^\circ \text{ yr}^{-1}$  ( $P < 0.01$ ), respectively. Importantly, forest loss in the mountains accounted for most of the observed increases in both mean elevation (64%;  $9.6 \pm 2.7 \text{ m yr}^{-1}$ ,  $P < 0.01$ ) and slope (64%;  $0.14 \pm 0.04^\circ \text{ yr}^{-1}$ ,  $P < 0.01$ ) after the IPs (Fig. 2a,b).

Regional patterns of trends in the mean elevation and slope where forest loss occurred (forest-loss topography) show that east Sumatra and Kalimantan (Indonesia), north Laos, and northeast Myanmar contribute to most of the increases in forest-loss topography after IPs (Fig. 2). In some regions, a decreasing trend in forest-loss topography occurred, such as on the Malay Peninsula (including southern Thailand and Malaysia) and in Vietnam (Supplementary Fig. 5). In Indonesia, which experienced the largest magnitude of forest loss (Supplementary Fig. 4), a sharp increase in forest-loss topography occurred during the second decade (Supplementary Fig. 5). These losses in Indonesia contribute to most of the increase in mean elevation (44% or  $6.6 \pm 1.6 \text{ m yr}^{-1}$ ,  $P < 0.01$ ) and slope (41% or  $0.09 \pm 0.03^\circ \text{ yr}^{-1}$ ,  $P < 0.01$ ) in SEA after the IPs (Fig. 2a,b). Also of regional importance were the increases in forest-loss topography in Laos (28% for SEA's elevation and 23% for SEA's slope) and

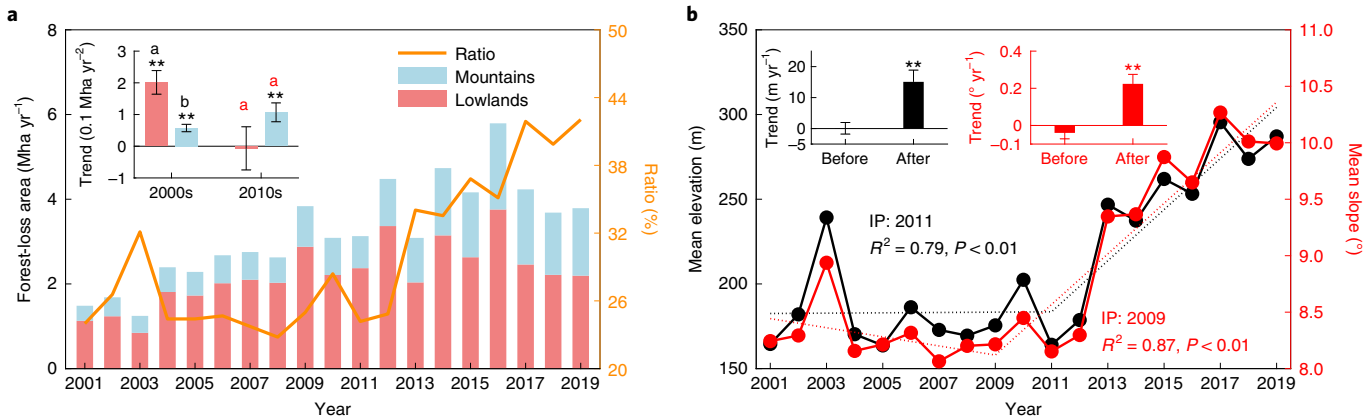


**Fig. 1 | Time series of forest-loss area and associated topography across SEA during the period 2001–2019.** **a**, Annual forest-loss area in the lowlands (pink bars) and mountains (blue bars) and the ratio of mountain forest-loss area to total forest-loss area (orange line). Inset bars show trends in lowland and mountain forest-loss area in the 2000s and 2010s. Different letters above the bars indicate statistically significant differences ( $P < 0.05$ ) between trends for lowlands and mountains during the 2000s (black letters) and 2010s (red letters). **b**, Mean elevation (solid black lines) and slope (solid red lines) of lands incurring forest loss. Dotted lines are trend lines for mean elevation (black) and slope (red) before and after IPs, which were estimated by piecewise regression. Inset bars show trends in mean elevation (black) and slope (red) before and after IPs. Error bars indicate the standard error of linear trends. \*Statistically significant trend at the level of  $P < 0.05$ ; \*\*statistically significant trend at the level of  $P < 0.01$ .

Myanmar (26% for SEA's elevation and 23% for SEA's slope). In other countries, such as Thailand and the Philippines, trends in forest-loss topography were comparatively small (Supplementary Fig. 5).

**Carbon loss resulting from forest clearance.** The observed shift in forest loss to higher elevations and steeper slopes is of concern because mountain forests in the region tend to have higher carbon stocks than lowland forests<sup>22</sup>:  $141 \pm 49 \text{ Mg Ch}^{-1}$  in the mountains versus  $101 \pm 69 \text{ Mg Ch}^{-1}$  in the lowlands (Supplementary Fig. 1). By incorporating the forest change calculations in the previous section with the forest carbon stock map<sup>21</sup> (Methods), we estimate the total forest carbon loss in SEA during 2001–2019 was 8,050 Tg, equivalent to a rate of  $424 \text{ Tg C yr}^{-1}$  (Fig. 3a and Table 1). As with annual forest loss, forest carbon stock loss increased continuously throughout the entire period, accelerating significantly at a rate of  $18 \pm 4 \text{ Tg C yr}^{-2}$  ( $P < 0.01$ ; Fig. 3a and Table 1). Nearly a third of the loss in forest carbon stocks (2,584 Tg C;  $136 \text{ Tg C yr}^{-1}$ ) occurred in the mountains; lowland forest carbon stock losses totalled 5,466 Tg (68%;  $288 \text{ Tg C yr}^{-1}$ ). Mountain forest carbon loss accelerated significantly in both the first ( $8 \pm 2 \text{ Tg C yr}^{-2}$ ,  $P < 0.01$ ) and second ( $10 \pm 4 \text{ Tg C yr}^{-2}$ ,  $P < 0.05$ ) decades, whereas the significant acceleration of lowland forest carbon stock loss in the first decade ( $27 \pm 5 \text{ Tg C yr}^{-2}$ ,  $P < 0.01$ ) was followed by a non-significant decrease in the 2010s ( $-9 \pm 8 \text{ Tg C yr}^{-2}$ ,  $P = 0.30$ ). These trends result in the increasing contribution of mountain forest carbon loss to total forest carbon loss in the second decade of the twenty-first century. Moreover, increasing clearance of mountain forests with dense carbon stocks results in a disproportionate loss of carbon stocks relative to past times when forest loss was more prevalent at lower elevations. For example, in 2019, the last year of the analysis, mountain forest carbon loss was  $119 \text{ Mg Ch}^{-1} \text{ yr}^{-1}$ , which was 7% higher than that of the lowlands. If these carbon-loss rate trajectories continue, annual forest carbon loss in the mountains will exceed that of lowlands by 2022.

In agreement with the forest-loss trends, the frontier of forest carbon loss also climbed to higher elevations and steeper slopes during 2001–2019 (Fig. 3b). However, there are stark regional differences in forest carbon-loss patterns with respect to topography (Fig. 4). In maritime SEA during the 2000s, most forest carbon losses took place in the lowlands (Fig. 4a), particularly on some Indonesian islands (for example, Sumatra, Kalimantan) and the

Malay Peninsula (Fig. 4c). Forest carbon loss in the lowlands of maritime SEA accounted for 65% of SEA's total carbon loss in the 2000s. In the 2010s, lowland forest carbon loss decreased, particularly in Sumatra and Kalimantan (Fig. 4d). However, positive trends in annual forest carbon loss occurred throughout many mountainous areas of mainland SEA, pushing upwards and accelerating in the mountains of Laos and Myanmar. Although forest and related carbon loss in Vietnam and the Malay Peninsula increased (Fig. 4b and Supplementary Fig. 4), the topography of forest loss in those regions decreased (Fig. 2 and Supplementary Fig. 5), indicating that forest (carbon) loss accelerated in regions with lower elevations, a pattern that is opposite to those observed in Myanmar and Laos. Overall, we conclude that the hotspots of forest carbon loss, while mirroring those of forest loss in general, were found predominantly in lowland maritime SEA in the 2000s. They were then located disproportionately in the mountains of mainland SEA in the 2010s, particularly in northern Laos and northeast Myanmar, locations strongly associated with increased forest loss at higher elevations and on steeper slopes (Fig. 2c,d).

## Discussion

In this section, we discuss the net changes in forest loss, implications and potential limitations that need to be further addressed in future studies. Finally, we summarize our findings.

**Net changes.** In the dynamic environments of SEA, forest losses were also counteracted to some degree by forest gains during the study in both lowland and mountain areas. Using the data developed by Hansen et al.<sup>8</sup>, we determine that forest gains during the period of 2001–2012 were  $10.3 \text{ Mha}$  ( $0.86 \text{ Mha yr}^{-1}$ ) in the lowlands and  $2.7 \text{ Mha}$  ( $0.23 \text{ Mha yr}^{-1}$ ) in the mountains (Supplementary Fig. 6). These gains result in the net-to-gross loss proportion of 56% and 66% in the lowlands and mountains, respectively, during this abbreviated period. The lower net-to-gross loss rate in the lowlands may be related to extensive oil palm and timber plantation establishment following the removal of forest or older plantations<sup>24</sup>, as maturing plantations would be counted as forest gain once plants exceed the threshold 5 m tree height definition of Hansen et al.<sup>8,25</sup>. By assuming that the net-to-gross loss ratios during 2013–2019 are the same as those in the earlier period, we estimate a  $23.6 \text{ Mha}$  ( $1.24 \text{ Mha yr}^{-1}$ ) net forest loss in the lowlands and a  $12.5 \text{ Mha}$  ( $0.66 \text{ Mha yr}^{-1}$ ) net

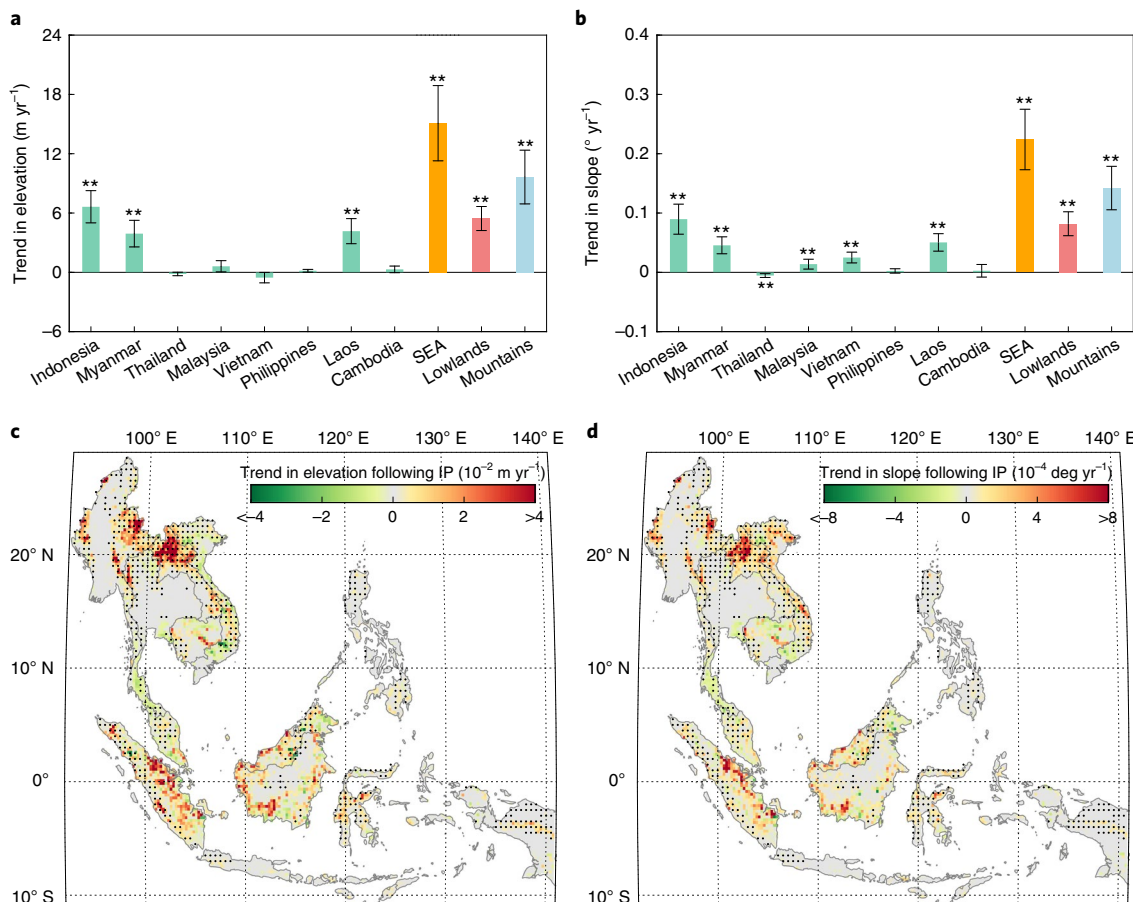


**Fig. 2 | Trends in mean elevation and slope of lands incurring forest loss following the IPs.** **a,b**, Trend in mean elevation (**a**) and slope (**b**) following the IPs in the eight countries of SEA (green bars), all of SEA (orange bars), lowlands (pink bars) and mountains (blue bars). Three countries in SEA (Brunei, East Timor and Singapore) are not presented here because their combined forest loss is only 0.2% of the SEA total. The error bars indicate the standard error of the linear trend. \*\*Statistically significant trend at the level of  $P < 0.01$ . **c,d**, Spatial patterns of trends in mean elevation (**c**) and slope (**d**) of lands incurring forest loss in 0.25° cells across SEA. Black dots indicate mountain regions. The IPs for mean elevation and slope are around 2011 and 2009, respectively (Fig. 1b). Trends in mean elevation and slope of lands incurring forest loss in each 0.25° cell or each country (or in the lowlands and mountains) were calculated considering the weight of forest loss using equations (1) and (2), respectively (Methods).

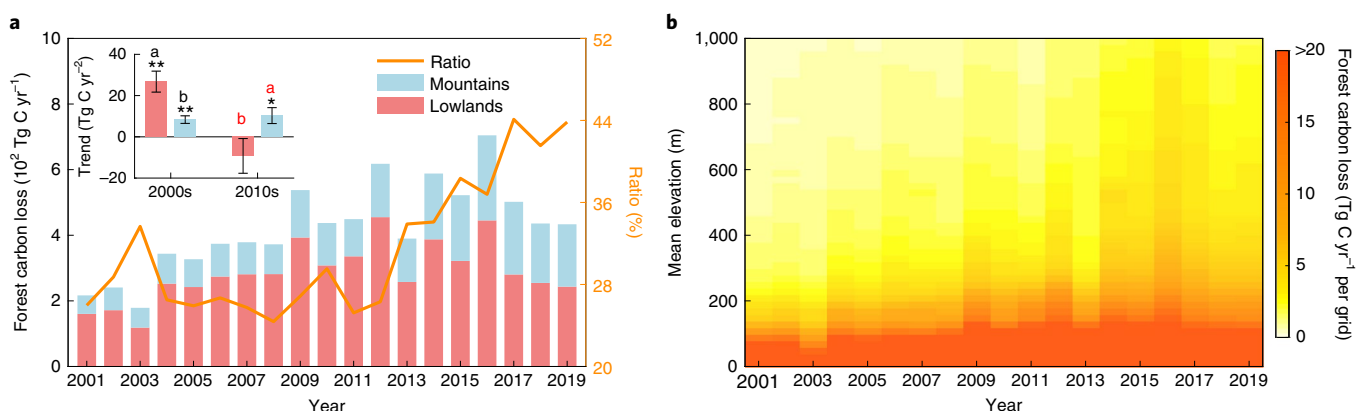


**Fig. 3 | Time series of forest carbon loss and associated topography across SEA during the period 2001–2019.** **a**, Annual forest carbon loss in the lowlands (pink bars) and mountains (blue bars) and the ratio of mountain forest carbon loss to total forest carbon loss (orange line). Inset bars show the trends in lowland and mountain forest carbon loss in the 2000s and 2010s. Error bars show the standard error of the linear trends. \*Statistically significant trend at the level of  $P < 0.05$ ; \*\*statistically significant trend at the level of  $P < 0.01$ . Different letters above the bars indicate statistically significant differences ( $P < 0.05$ ) between trends for lowlands and mountains during the 2000s (black letters) and 2010s (red letters). **b**, Carbon loss in elevation–year space.

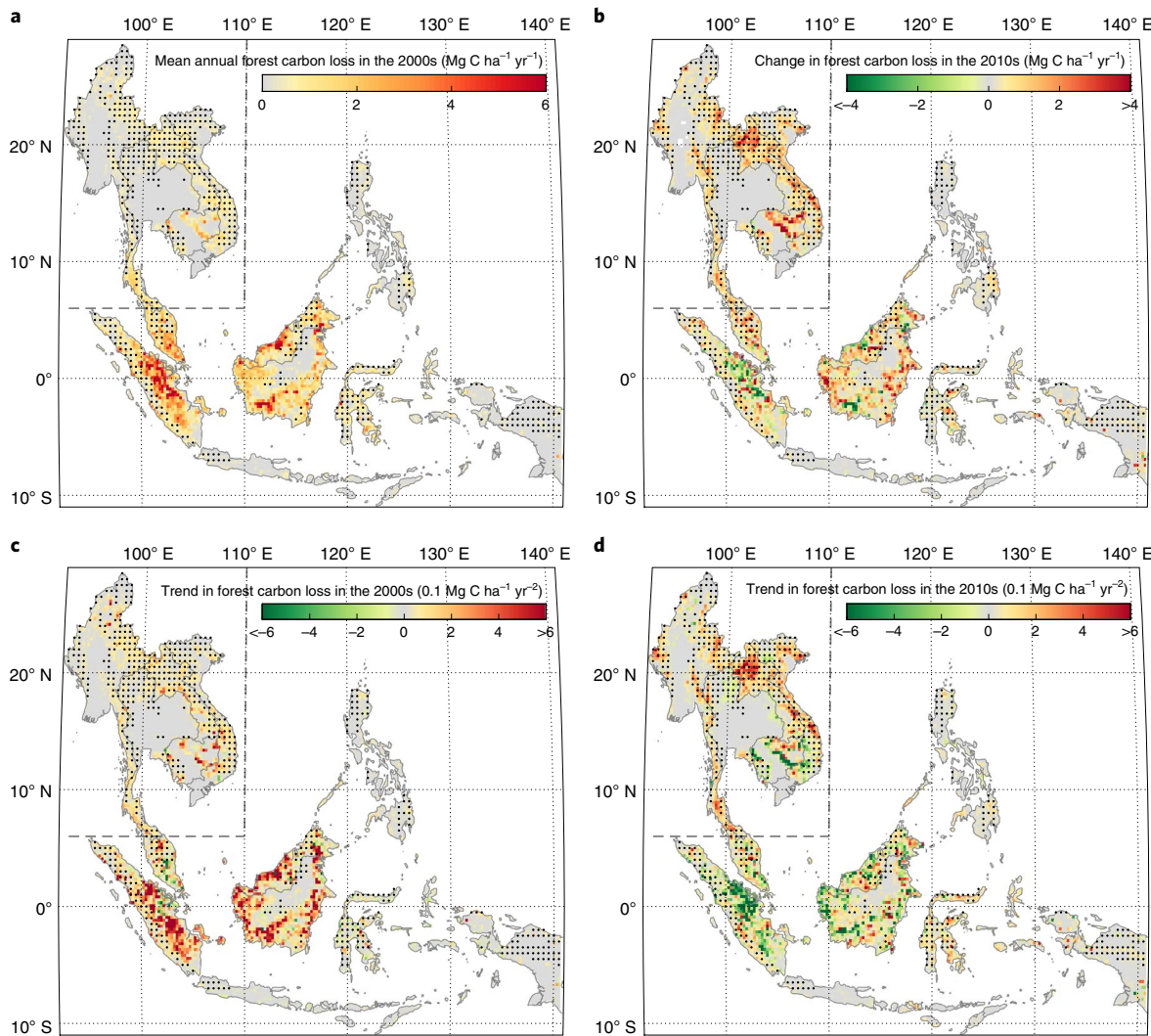


**Fig. 4 | Spatial patterns of forest carbon loss across SEA during the period 2001–2019.** **a**, Mean annual forest carbon loss in the 2000s. **b**, Change in mean annual forest carbon loss in the 2010s relative to the 2000s. **c,d**, Trend in mean annual forest carbon loss in the 2000s (**c**) and 2010s (**d**). Grey dashed lines show mainland SEA (inside the box) and maritime SEA (outside the box). Black dots indicate mountain regions.

forest loss in the highlands during 2001–2019 (Supplementary Fig. 6). These estimates of net loss are probably conservative, given that forest loss accelerated at a rate of  $0.17 \pm 0.03 \text{ Mg ha}^{-1} \text{ yr}^{-2}$  ( $P < 0.01$ ) throughout the entire period (Table 1).

Overall, our net estimates also reveal a clear fingerprint of mountain forest loss that is accelerating in some countries of SEA (for example, Indonesia, Myanmar, and Laos) during the early twenty-first century, due primarily to expansion of agriculture for crop plantation<sup>19,20</sup>. The accelerating mountain forest loss in the 2010s, originated from secondary forest loss, mirrors the replacement of swidden fields with other agriculture systems. For example, a notable shift from swidden fields, where secondary forests regenerate during fallow period, to permanent agriculture systems is reported in the mountains of Laos<sup>26</sup>, indicating that these forest losses in the mountains of SEA are partly a result of agriculture intensification. This pattern, however, is different from agricultural expansion in the Midwestern United States, which made the farms in the northeastern United States not profitable and hence resulted in forest regeneration in that region<sup>27</sup>.

**Implications.** Our results demonstrate not only a continuation of forest loss in SEA as reported in sub-regions during previous periods<sup>6,9</sup>,

but also an acceleration in loss that includes encroachment into forests at higher elevations with higher carbon density. These trends influence the roles tropical forests play in the context of global climate mitigation, biodiversity conservation and global carbon cycling. For example, the observed acceleration in forest carbon loss counters efforts to limit global warming to below 2 °C by the end of this century<sup>28</sup>. The climb in the forest-loss frontier also represents a challenge for climate change assessments as current Earth system models do not differentiate mountain from lowland forest loss because of their coarse spatial resolutions<sup>19</sup>, potentially resulting in the misrepresentation of climate feedbacks. In addition to the warming triggered by forest carbon loss to the atmosphere through biochemical feedbacks, tree replacement increases surface temperature at a variety of scales through biophysical feedbacks<sup>28,29</sup>. In the mountains of SEA, where most deforested lands are converted to croplands<sup>19</sup>, warming effects related to forest loss tend to be amplified due to suppressed evapotranspiration, raising local temperatures by up to 2 °C<sup>29–31</sup>. The acceleration of mountain forest loss in the region has probably already enhanced these warming effects and influenced the carbon budget.

The acceleration in forest loss also affects biodiversity conservation in the region because a great number of endemic species are

found in the mountains of SEA<sup>32</sup>. While widespread conversion of forests to croplands substantially reduces species richness and alters community composition in general, loss of mountain forest habitat is particularly detrimental<sup>33,34</sup>. Tropical montane species typically live within specific hydro-thermal environments, which are dramatically altered during forest conversion, increasing extinction risk<sup>35,36</sup>. Deforestation also interacts with climate changes, forcing species to redistribute<sup>37</sup>, often to higher and cooler locations. Mountain forest loss threatens to reduce the area of suitable habitat to accommodate these types of relocations<sup>38</sup>.

Beyond the direct loss of carbon associated with vegetation biomass removal and habitat loss, forest loss also affects the carbon cycle through diminishing photosynthesis and altering soil carbon stocks. For example, forest loss directly lowers landscape-wide photosynthesis due to decreases in leaf area and alteration of vegetation functioning. Forest conversion also alters basic water-balance processes, including evapotranspiration, infiltration and water storage<sup>39–41</sup>, thereby modulating vegetation growth and associated carbon assimilation. Soil erosion accelerated by forest conversion, particularly on sloping lands, exhumes soil carbon that may be quickly released to the atmosphere or transported into downslope flood-plain locations, water bodies or the ocean, where it is stored/lost at variable timescales<sup>42,43</sup>. Unfortunately, because of the absence of regional data on soil carbon stocks, we were not able to account for losses of this component, which for some forest conversion outcomes are substantial<sup>3,44</sup>.

**Uncertainties and caveats.** With regard to uncertainties in our analysis, fragmentation and edge effects of forest losses can alter microclimates and thus regulate the growth and structure of nearby trees, causing additional long-term carbon losses on the landscape that we could not quantify<sup>45</sup>. Additional uncertainty relates to our inability to detect forest conversions at scales smaller than a Landsat pixel, for example, those related to small-scale, fallow-based swidden agriculture, which is still practiced in some areas of SEA<sup>20,46</sup>. Again, our estimates also represent absolute forest carbon losses, not net losses that incorporate biomass carbon gains that could not be calculated from available data with confidence. Even with these uncertainties in mind, the acceleration of loss in mountain forests with high carbon density that we find on the basis of immediate vegetative biomass changes alone portends additional redistributions and losses of carbon in the near future, potentially nudging SEA's forests to be a net carbon source in the global carbon budget<sup>45,47</sup> rather than a neutral actor<sup>5</sup>. To reduce these uncertainties, future studies could integrate higher-resolution satellite and lidar datasets to map primary and secondary forests and related biomass carbon loss more accurately. More studies on above- and belowground carbon recovery associated with forest regrowth are also needed.

In summary, our results reveal changing topographical patterns associated with forest loss in SEA during the first two decades of the twenty-first century. The shift is characterized by an upward expansion in the frontier of forest exploitation, from occurring predominantly in the lowlands to increasingly encroaching forests at higher elevations with comparatively higher carbon stocks and more-sensitive species. The acceleration of this trend throughout the two decades provides new insight regarding forest and carbon dynamics in the region that has not been recognized in previous climate change assessments or parameterized in current model configurations simulating impacts. Such exclusion misrepresents regional biophysical and biochemical feedbacks of deforestation. Collectively, knowledge of the ascent of the frontier of forest loss across SEA is needed to develop effective policies to manage concomitant negative impacts on biodiversity, water resources, land degradation and the carbon cycle. This knowledge is valuable for developing strategies to reduce future losses of remaining forests that still have great ability to preserve valuable ecosystem services,

including atmospheric carbon dioxide capture and biodiversity conservation.

## Methods

This section provides details on the datasets and methods used for quantifying changes in topographical patterns of forest clearance and related carbon loss across SEA.

**High-resolution forest-cover change and primary forest extent products.** To quantify forest-cover change over SEA from 2001 to 2019, we used a high-resolution remote sensing product that maps tree-cover change at a spatial resolution of 30 m (version 1.7; ref. <sup>8</sup>). The dataset has user's and producer's accuracies of >83% over the tropics<sup>8</sup>. A previous independent assessment indicated that, in SEA, the data have user's and producer's accuracies of 93.2% and 81.2%, respectively<sup>19</sup>. This dataset defines trees as “all vegetation taller than 5 m in height”, and forest loss (including via deforestation and forest degradation) as “the mortality or removal of all tree cover within a 30 m pixel”<sup>8,25</sup>. This operational definition results in the case that planted vegetation, such as rubber and oil palm plantations, is mapped as trees when taller than 5 m. Removal of such vegetation is counted as tree-cover loss. Following these definitions, the data provide maps of forest-cover loss and the year of loss during 2001–2019 and forest-cover gain during 2001–2012. Forest loss across SEA exhibits a continuous increase trend from 2001 to 2019, confirming that changes in the loss-detection method do not dominate the long-term trend. To separate forest-loss type, we further used a dataset on the extent of primary forests at 30 m spatial resolution for the year 2001 in SEA<sup>10</sup>.

**Topography data.** We used both mountain-extent maps and a digital elevation model to quantify the topographic pattern of forest loss. Mountain extent in SEA was mapped by a series of mountain polygons developed by the Global Mountain Biodiversity Assessment (GMBA) inventory (version 1.2; ref. <sup>18</sup>). The GMBA inventory defines a 2.5-arcmin pixel as mountainous if the geometrical amplitude between the highest and lowest elevation exceeds 200 m. Following this definition, there are 61 mountain regions in SEA (Supplementary Fig. 2a), occupying 1.7 million km<sup>2</sup> (38%) of SEA's land surface. The remaining 62% of SEA's land surface is treated as lowland. The associated elevation information in the lowlands and mountains, at a spatial resolution of 30 m, is collected from the Advanced Spaceborne Thermal Emission and Reflection Radiometer Global Digital Elevation Model (version 3; ref. <sup>48</sup>). Slope information is estimated from elevation data using the average maximum method<sup>19</sup>.

**Forest carbon stocks.** We calculated forest carbon losses by incorporating the high-resolution AGB density map of Zarin et al.<sup>21</sup> into our analyses of forest loss. The map represents AGB density (in a unit of Mg per hectare of biomass) at a spatial resolution of 30 m circa 2000. The AGB map was generated using a random forest model and a statistical model from measured forest biomass, the Geoscience Laser Altimeter System lidar data and gridded variables such as Landsat 7 Enhanced Thematic Mapper Plus reflectance and biophysical variables, such as precipitation<sup>21</sup>. Due to lack of data, we estimate belowground biomass (BGB) at the pixel level with the empirical allometric model of Mokany et al.<sup>50</sup> that has been widely used for BGB estimations<sup>2,51</sup>:  $BGB = 0.489 \times AGB^{0.89}$ . Total forest vegetation biomass, calculated as the sum of AGB and BGB, was converted to total forest biomass carbon stocks using a conversion factor of 0.5 (refs. <sup>2,21</sup>).

**Forest- and carbon-loss calculations and analysis.** We estimated forest-loss area by summing the areas of forest-loss pixels that are dependent on their geographical location<sup>45</sup>. The area of forest carbon loss was calculated by overlapping the forest-loss data with the forest carbon stock density map (including aboveground and belowground). We used committed emissions of carbon from forests to the atmosphere on forest loss, even though some of the carbon associated with tree removal degrades on site or over time or is embedded within wood products<sup>15</sup>.

As both forest-loss area and forest carbon loss showed near-uniform increases over time, we applied a simple least-squares linear regression model to quantify the rate of change (Figs. 1a and 3a and Supplementary Figs. 4 and 5). By contrast, because trends in mean elevation and slope of lands incurring forest loss in the 2000s and 2010s were nonlinear (Fig. 1b), we used a piecewise linear regression model<sup>52–54</sup> to (1) determine where the trends in the time series of mean elevation and slope change (IPs) and (2) quantify the trends before and after the IPs. We also used a statistical model in Real Statistics Resource Pack to test whether the differences in trends between mountain forest (carbon) loss and lowland forest (carbon) loss was statistically significant<sup>55</sup>.

To demonstrate the spatial pattern of increases following IPs, we separated them into each 0.25° cell and used the equations:

$$H_{t,k} = \frac{\sum \bar{h}_{s_t} + h_{t,k} s_{t,k}}{\sum s_t + s_{t,k}} \quad (1)$$

$$I_{t,k} = \frac{\sum \bar{i}_{s_t} + i_{t,k} s_{t,k}}{\sum s_t + s_{t,k}} \quad (2)$$

where  $H_{t,k}$  and  $I_{t,k}$  are the mean elevation and slope in year  $t$  for the  $k$ th  $0.25^\circ$  cell;  $\bar{h}$  (245.5 m) and  $\bar{i}$  (9.3°) are the mean elevation and slope of forest loss across SEA after IPs, respectively;  $s_{t,k}$  and  $s_t$  are forest-loss area in year  $t$  for the  $k$ th  $0.25^\circ$  cell and other cells, respectively. While the elevation and slope data for other cells are assumed to be the means of SEA ( $\bar{h}$  and  $\bar{i}$ ), the elevation and slope data for the  $k$ th  $0.25^\circ$  cell are realistic. Thus, trends in the time series after IPs are caused by the changes only in the  $k$ th  $0.25^\circ$  cell. We then used a piecewise linear regression model to calculate trends in mean elevation and slope before and after identified IPs. Following this method, we calculated the trends caused by each cell for countries (by summing all cells in each country), mountains (by summing all cells in the mountains) and lowlands (by summing all cells in the lowlands).

## Data availability

The global maps of forest-cover loss and gain are available at [https://earthenginepartners.appspot.com/science-2013-global-forest/download\\_v1.7.html](https://earthenginepartners.appspot.com/science-2013-global-forest/download_v1.7.html). The ASTER elevation data are available at <https://earthdata.nasa.gov>. The GMBA inventory is available at [https://ilias.unibe.ch/goto\\_ilias3\\_unibe\\_cat\\_1000515.html](https://ilias.unibe.ch/goto_ilias3_unibe_cat_1000515.html). The aboveground biomass maps are available at <https://www.globalforestwatch.org/map/global/>. The primary extent data are available at <https://glad.umd.edu/dataset/primary-forest-humid-tropics>. All datasets are also available upon request from the corresponding author.

## Code availability

The scripts used to generate all the results are MATLAB (R2020a). Analysis scripts are available at <https://doi.org/10.6084/m9.figshare.14586528>.

Received: 29 January 2021; Accepted: 30 May 2021;

Published online: 28 June 2021

## References

1. Bonan, G. B. Forests and climate change: forcings, feedbacks, and the climate benefits of forests. *Science* **320**, 1444–1449 (2008).
2. Saatchi, S. S. et al. Benchmark map of forest carbon stocks in tropical regions across three continents. *Proc. Natl Acad. Sci. USA* **108**, 9899–9904 (2011).
3. Veldkamp, E., Schmidt, M., Powers, J. S. & Corre, M. D. Deforestation and reforestation impacts on soils in the tropics. *Nat. Rev. Earth Environ.* **1**, 590–605 (2020).
4. Ceccherini, G. et al. Abrupt increase in harvested forest area over Europe after 2015. *Nature* **583**, 72–77 (2020).
5. Mitchard, E. T. A. The tropical forest carbon cycle and climate change. *Nature* **559**, 527–534 (2018).
6. Curran, L. M. et al. Lowland forest loss in protected areas of Indonesian Borneo. *Science* **303**, 1000–1003 (2004).
7. Friedl, A. et al. *MODIS Collection 5 Global Land Cover: Algorithm Refinements and Characterization of New Datasets, 2001–2012 Collection 5.1* (Boston University, 2010).
8. Hansen, M. C. et al. High-resolution global maps of 21st-century forest cover change. *Science* **342**, 850–853 (2013).
9. Margono, B. A., Potapov, P. V., Turubanova, S., Stolle, F. & Hansen, M. C. Primary forest cover loss in Indonesia over 2000–2012. *Nat. Clim. Change* **4**, 730–735 (2014).
10. Turubanova, S. et al. Ongoing primary forest loss in Brazil, Democratic Republic of the Congo, and Indonesia. *Environ. Res. Lett.* **13**, 074028 (2018).
11. Searchinger, T. et al. *Creating a Sustainable Food Future: A Menu of Solutions to Feed Nearly 10 Billion People by 2050* (World Resources Institute, 2019).
12. Gibbs, H. K. et al. Tropical forests were the primary sources of new agricultural land in the 1980s and 1990s. *Proc. Natl Acad. Sci. USA* **107**, 16732–16737 (2010).
13. Tyukavina, A. et al. Congo Basin forest loss dominated by increasing smallholder clearing. *Sci. Adv.* **4**, eaat2993 (2018).
14. Achard, F. et al. Determination of tropical deforestation rates and related carbon losses from 1990 to 2010. *Glob. Change Biol.* **20**, 2540–2554 (2014).
15. Baccini, A. et al. Tropical forests are a net carbon source based on aboveground measurements of gain and loss. *Science* **358**, 230–234 (2017).
16. Aide, T. M. et al. Woody vegetation dynamics in the tropical and subtropical Andes from 2001 to 2014: satellite image interpretation and expert validation. *Glob. Change Biol.* **25**, 2112–2126 (2019).
17. Song, X. P. et al. Global land change from 1982 to 2016. *Nature* **560**, 639–643 (2018).
18. Körner, C. et al. A global inventory of mountains for bio-geographical applications. *Alp. Bot.* **127**, 1–15 (2017).
19. Zeng, Z. et al. Highland cropland expansion and forest loss in Southeast Asia in the twenty-first century. *Nat. Geosci.* **11**, 556–562 (2018).
20. Zeng, Z., Gower, D. B. & Wood, E. F. Accelerating forest loss in Southeast Asian Massif in the 21st century: a case study in Nan Province, Thailand. *Glob. Change Biol.* **24**, 4682–4695 (2018).
21. Zarin, D. J. et al. Can carbon emissions from tropical deforestation drop by 50% in 5 years? *Glob. Change Biol.* **22**, 1336–1347 (2016).
22. Spracklen, D. & Righelato, R. Tropical montane forests are a larger than expected global carbon store. *Biogeosciences* **11**, 2741–2754 (2014).
23. Miettinen, J., Shi, C. & Liew, S. C. Deforestation rates in insular Southeast Asia between 2000 and 2010. *Glob. Change Biol.* **17**, 2261–2270 (2011).
24. Austin, K. G. et al. What causes deforestation in Indonesia? *Environ. Res. Lett.* **14**, 024007 (2019).
25. Hansen, M. et al. Response to comment on ‘high-resolution global maps of 21st-century forest cover change’. *Science* **344**, 981–981 (2014).
26. Chan, N., Xayvongsa, L. & Takeda, S. in *Environmental Resources Use and Challenges in Contemporary Southeast Asia* (eds Lopez, M. I. & Suryomenggolo, J.) 231–246 (Springer, 2018).
27. Thompson, J. R., Carpenter, D. N., Cogbill, C. V. & Foster, D. R. Four centuries of change in northeastern United States forests. *PLoS ONE* **8**, e72540 (2013).
28. Lawrence, D. & Vandecar, K. Effects of tropical deforestation on climate and agriculture. *Nat. Clim. Change* **5**, 27–36 (2015).
29. Zeng, Z. et al. Deforestation-induced warming over tropical mountain regions regulated by elevation. *Nat. Geosci.* **14**, 23–29 (2021).
30. Senior, R. A., Hill, J. K., Benedick, S. & Edwards, D. P. Tropical forests are thermally buffered despite intensive selective logging. *Glob. Change Biol.* **24**, 1267–1278 (2018).
31. Senior, R. A., Hill, J. K., González del Pliego, P., Goode, L. K. & Edwards, D. P. A pantropical analysis of the impacts of forest degradation and conversion on local temperature. *Ecol. Evol.* **7**, 7897–7908 (2017).
32. Sodhi, N. S. et al. The state and conservation of Southeast Asian biodiversity. *Biodivers. Conserv.* **19**, 317–328 (2010).
33. Ahrends, A. et al. Current trends of rubber plantation expansion may threaten biodiversity and livelihoods. *Glob. Environ. Change* **34**, 48–58 (2015).
34. Edwards, D. P. et al. Degraded lands worth protecting: the biological importance of Southeast Asia’s repeatedly logged forests. *Proc. R. Soc. B* **278**, 82–90 (2011).
35. Srinivasan, U., Elsen, P. R. & Wilcove, D. S. Annual temperature variation influences the vulnerability of montane bird communities to land-use change. *Ecosystems* **42**, 2084–2094 (2019).
36. Rahbek, C. et al. Humboldt’s enigma: what causes global patterns of mountain biodiversity? *Science* **365**, 1108–1113 (2019).
37. Guo, F., Lenoir, J. & Bonebrake, T. C. Land-use change interacts with climate to determine elevational species redistribution. *Nat. Commun.* **9**, 1315 (2018).
38. Elsen, P. R., Monahan, W. B. & Merenlender, A. M. Topography and human pressure in mountain ranges alter expected species responses to climate change. *Nat. Commun.* **11**, 1974 (2020).
39. Spracklen, D. V., Arnold, S. R. & Taylor, C. M. Observations of increased tropical rainfall preceded by air passage over forests. *Nature* **489**, 282–285 (2012).
40. Spracklen, D. V. & Garcia-Carreras, L. The impact of Amazonian deforestation on Amazon Basin rainfall. *Geophys. Res. Lett.* **42**, 9546–9552 (2015).
41. Cheng, L. et al. Quantifying the impacts of vegetation changes on catchment storage–discharge dynamics using paired-catchment data. *Water Resour. Res.* **53**, 5963–5979 (2017).
42. Chappell, A., Baldock, J. & Sanderman, J. The global significance of omitting soil erosion from soil organic carbon cycling schemes. *Nat. Clim. Change* **6**, 187–191 (2015).
43. Yue, Y. et al. Lateral transport of soil carbon and land–atmosphere  $\text{CO}_2$  flux induced by water erosion in China. *Proc. Natl Acad. Sci. USA* **113**, 6617–6622 (2016).
44. Ziegler, A. D. et al. Carbon outcomes of major land-cover transitions in SE Asia: great uncertainties and REDD+ policy implications. *Glob. Change Biol.* **18**, 3087–3099 (2012).
45. Brinck, K. et al. High resolution analysis of tropical forest fragmentation and its impact on the global carbon cycle. *Nat. Commun.* **8**, 14855 (2017).
46. Fox, J., Castella, J. C. & Ziegler, A. D. Swidden, rubber and carbon: can REDD+ work for people and the environment in montane mainland Southeast Asia? *Glob. Environ. Change* **29**, 318–326 (2014).
47. Harris, N. L. et al. Global maps of twenty-first century forest carbon fluxes. *Nat. Clim. Change* <https://doi.org/10.1038/s4158-020-00976-6> (2021).
48. Tachikawa, T., Hato, M., Kaku, M. & Iwasaki, A. Characteristics of ASTER GDEM version 2. In *Proc. IEEE International Geoscience and Remote Sensing Symposium (IGARSS)* 3657–3660 (IEEE, 2011).
49. Burrough, P. A., McDonnell, R., McDonnell, R. A. & Lloyd, C. D. *Principles of Geographical Information Systems* (Oxford Univ. Press, 2015).
50. Mokany, K., Raison, R. J. & Prokushkin, A. S. Critical analysis of root : shoot ratios in terrestrial biomes. *Glob. Change Biol.* **12**, 84–96 (2006).
51. Tyukavina, A. et al. Aboveground carbon loss in natural and managed tropical forests from 2000 to 2012. *Environ. Res. Lett.* **10**, 074002 (2015).
52. Ryan, S. E. & Porth, L. S. *A Tutorial on the Piecewise Regression Approach Applied to Bedload Transport Data* (CreateSpace, 2015).
53. Toms, J. D. & Lesperance, M. L. Piecewise regression: a tool for identifying ecological thresholds. *Ecology* **84**, 2034–2041 (2003).

54. Zeng, Z. et al. A reversal in global terrestrial stilling and its implications for wind energy production. *Nat. Clim. Change* **9**, 979–985 (2019).
55. Zaiontz, C. *Real Statistics Using Excel* (accessed 16 June 2021); <http://www.real-statistics.com/>

### Acknowledgements

Z.Z. and C.Z. were supported by the National Natural Science Foundation of China (grant nos. 42071022, 41861124003 and 41890852). Z.Z. was also supported by the start-up fund provided by Southern University of Science and Technology (no. 29/Y01296122). We thank Hansen/UMD/Google/USGS/NASA for providing the high-resolution forest change and primary forest extent data; NASA and Japan's Ministry of Economy, Trade and Industry for providing the elevation data; Körner for providing the GMBA inventory; and Zarin/WHRC for providing the aboveground biomass density maps.

### Author contributions

Z.Z. designed the research; Y.F. performed the analysis; Y.F. and A.D.Z. wrote the draft. All authors contributed to the interpretation of the results and the writing of the paper.

### Competing interests

The authors declare no competing interests.

### Additional information

**Supplementary information** The online version contains supplementary material available at <https://doi.org/10.1038/s41893-021-00738-y>.

**Correspondence and requests for materials** should be addressed to Z.Z.

**Peer review information** *Nature Sustainability* thanks Stephen Leisz, Ensheng Weng, and the other, anonymous, reviewer(s) for their contribution to the peer review of this work.

**Reprints and permissions information** is available at [www.nature.com/reprints](http://www.nature.com/reprints).

**Publisher's note** Springer Nature remains neutral with regard to jurisdictional claims in published maps and institutional affiliations.

© The Author(s), under exclusive licence to Springer Nature Limited 2021